Design of Planar and Conformal Frequency Selective Surface as Filter: For Radome Wireless Communication

A DISSERTATION
SUBMITTED IN PARTIAL FULFILLMENT OF THE REQUIREMENTS
FOR THE AWARD OF THE DEGREE
OF

MASTER OF TECHNOLOGY
IN
SIGNAL PROCESSING & DIGITAL DESIGN

Submitted by:
SANJEETA DHEGAYA
2K20/SPD/17

Under the supervision of
MS. LAVI TANWAR

DEPARTMENT OF ELECTRONICS AND COMMUNICATION ENGINEERING
DELHI TECHNOLOGICAL UNIVERSITY
(Formerly Delhi College of Engineering)
Bawana Road, Delhi-110042

May, 2022

DEPARTMENT OF ELECTRONICS AND COMMUNICATION ENGINEERING

DELHI TECHNOLOGICAL UNIVERSITY

(Formerly Delhi College of Engineering)
Bawana Road, Delhi-110042

CANDIDATE'S DECLARATION

I **Sanjeeta Dhegaya, Roll No. 2K20/SPD/17** student of M.TECH (**SIGNAL PROCESSING & DIGITAL DESIGN**), hereby declare that the Project Dissertation titled "**Design of Planar and Conformal Frequency Selective Surface as Filter: For Radome Wireless Communication**" which is submitted by me to the Department of Electronics and Communication Engineering, Delhi Technological University, Delhi in partial fulfillment of the requirement for the award of the degree of Master of Technology, is original and not copied from any source without proper citation. This work has not previously formed the basis for the award of any Degree, Diploma Associateship, Fellowship or other similar title or recognition.

Place: Delhi **SANJEETA DHEGAYA**

Date: 24/05/2022

DEPARTMENT OF ELECTRONICS AND COMMUNICATION ENGINEERING

DELHI TECHNOLOGICAL UNIVERSITY

(Formerly Delhi College of Engineering)
Bawana Road, Delhi-110042

CERTIFICATE

I hereby certify that the Project Dissertation titled "**Design of Planar and Conformal Frequency Selective Surface as Filter: For Radome Wireless Communication**" which is submitted by **SANJEETA DHEGAYA**, **2K20/SPD/17** of Electronics and Communication Department, Delhi Technological University, Delhi in partial fulfillment of the requirement for the award of the degree of Master of Technology, is a record of the project work carried out by the student under my supervision. To the best of my knowledge this work has not been submitted in part or full for any Degree or Diploma to this University or elsewhere.

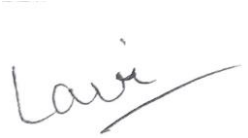

Place: Delhi

Date: 24/05/2022

MS. LAVI TANWAR

SUPERVISOR

ACKNOWLEDGEMENT

A successful project can never be prepared by the efforts of the person to whom the project is assigned, but it also demands the help and guardianship of people who helped in completion of the project. I would like to thank all those people who have helped me in this research and inspired me during my study. With profound sense of gratitude, I thank **Ms. Lavi Tanwar**, my Research Supervisor, for her encouragement, support, patience and her guidance in this research work.

Furthermore, I would also like to thank **Prof. N. S. RAGHAVA**, who gave me the permission to use all required equipment and the necessary format to complete the report.

I take immense delight in extending my acknowledgement to my family and friends who have helped me throughout this research work.

SANJEETA DHEGAYA

ABSTRACT

One of the major sources of radar cross section (RCS) in the frontal sector of the Aircraft is the Radome section. Radome is made of dielectric material which contributes to the RCS by the antenna used for surveillance and communication purposes. To counter this effect, a band-pass filter of frequency selective surface (FSS) is proposed with the dielectric substrate affecting the performance of a filter in the context of the resonant frequency. First influence of the dielectric layer on FSS element is analyzed then the insertion effect of planar, conformal FSS on antenna performance followed by proposed design of dual band-pass and band-stop FSS for wireless communication through CEM software is done.

Initially effect of dielectric layer insertion on frequency selective surface element as band-pass filter is analyzed keeping resonant frequency stable. As seen that the real-time structures are not always found to be planar, structures may be conformal with a different angle. To meet the real-time scenario both planar and conformal structures are presented. The past researches have some advantages but face some challenges too like maintenance and application in the conformal airborne platform. To meet this requirement simple unit cell FSS element is taken and the simulation is performed with a horn antenna in CST software. The material used is FR-4 with a dielectric constant of 4.3. The size of designed unit cell FSS both Square slot and Cross dipole slot are $0.32\lambda_0 \times 0.32\lambda_0$ and thickness of $0.0256\lambda_0$, where λ_0 is the resonant frequency. The results obtained is a single transmission pole with a band-width of 2.38 GHz and 0.86 GHz for Square slot and Cross dipole slot respectively at various incidence angles. The frequency selective surface element is replicated on the planar and conformal structure as a 3×3 FSS element array to observe the gain of the antenna with FSS. For observing the effectiveness of the filter throughout the frequency band of interest, the Insertion loss and gain of the antenna with FSS are analyzed. Maintaining the stable gain the performance of the antenna is analyzed

when frequency selective surfaces are inserted as a band-pass filter, for both planar and conformal structures.

Finally using two FSS elements .i.e. two square slots with a center square patch and two cross dipole patches diagonally arranged is designed in a two-dimensional unit cell for wireless application. The designed unit cell is used to obtain two transmission poles and one transmission zero for good isolation. This design is a single layer tri-band frequency selective surface. Two band-pass filters is at resonant frequency 6.04 GHz and 9.60 GHz with a band-width of 0.89 GHz and 0.87 GHz respectively. One stop band filter at resonant frequency 7.6 GHz in between the C-band and X-band plays an important role in good isolation for wireless communication. The size of unit cell FSS is $0.40\lambda_0 \times 0.40\lambda_0$ and the thickness of $0.016\lambda_0$, where λ_0 is the first lower resonant frequency. Both pass-band resonant frequencies are spaced with a good shielding providing the frequency ratio of 1.57.

Frequency selective surface element and dielectric material are examined through unit cell using floquet boundaries analysis method with the help of 3D EM Computational software. In view of this, in this project optimization of the insertion effect of dielectric substrate and designed FSS element is realized at an oblique incidence angle for both TE and TM polarization.

List of Acronyms

ACRONYM	DESCRIPTION
CAD	Computer Aided Design
CST	Computer Simulated Technology
CEM	Computational Electromagnetics
ECM	Equivalent Circuit Model
EM	Electro-Magnetics
ENZ	Epsilon Near Zero
FSS	Frequency Selective Surfaces
FR4	Flame Retardant
PTFE	Polytetrafluoroethylene
RCS	Radar Cross Section
RAM	Radar Absorber Material
SIW	Substrate Integrated Waveguide
SS-FSS	Square Slot Frequency selective surfaces
TE	Transverse Electric
TM	Transverse Magnetic

List of Figures

List of Tables

Table of Contents

1 INTRODUCTION

Frequency Selective Surface (FSS) is an array of repeated metallic elements with a dielectric substrate for mechanical support. From various surveys and research done earlier, it is evident that the study related to frequency selective surface [1] plays a vital role in the ease of development of various possibilities in the application area of filters, absorbers, radar cross section reduction, shielding, etc. FSS is typically a periodic element structure and can be used as filters [1] or absorbers [1], as used in traditional methods in circuit theory [2]. There are two main applications for the FSS structure. FSS can be used as spatial frequency filters in radome etc. or absorbing material in application area of a stealth platform [3, 4]. To make the aircraft stealthy frontal area .i.e. radome plays an important role which is made up of dielectric material [3, 4].

Dielectric Insertion effect on Frequency Selective Surfaces for Band Pass Filter design is observed as it not only provides mechanical support but also effect the shifting of the resonant frequency. Radome is made up of dielectric material which contributes to the RCS by the antenna and thus is highly visible to enemy radar (surface to air mode) or other enemy aircraft (air to air mode). It allows all EM energy to enter the dielectric radome raising the RCS of aircraft to a high level. To counter this effect, a band-pass filter of frequency selective surface is proposed with a dielectric substrate affecting the performance of a filter in the context of the resonant frequency. Simulation with a resonant frequency between 8 GHz to 12 GHz is examined. Effect of dielectric layer on frequency selective surface element is analyzed keeping stable resonant frequency.

To meet the real-time scenario both planar and conformal structures are presented. The real-time structures are not always found to be planar, structures may be conformal with different angles. To meet this requirement simple unit cell FSS element is taken and the simulation is performed with a horn antenna in CST software. The past researches have some advantages but face some challenges too like maintenance and application area in conformal airborne platform. With the increase of complexity in the design of the structure related to the airborne platform it is best to

opt for the simple solution. Thus, the performance of the antenna maintaining the stable gain is analyzed when frequency selective surfaces are used as a band-pass filter, both for planar and conformal structure. The results obtained are a single transmission pole with a band-width of 2.38 GHz and 0.86 GHz for the two designed unit cell FSS .i.e. Square slot and Cross dipole slot at various incidence angles. The material used is FR-4 with a dielectric constant of 4.3. The size of both designed unit cell FSS is $0.32\lambda_0 \times 0.32\lambda_0$ and the thickness of $0.0256\lambda_0$, where λ_0 is the resonant frequency. The unit cell FSS element is replicated on the planar and conformal structure as a 3×3 FSS element array to observe the gain of the antenna with FSS as a performance parameter. For observing the effectiveness of the filter throughout the frequency band of interest, the Insertion loss and gain of the antenna with FSS are analyzed.

Finally using two square slots with a center square patch and two cross dipole patches diagonally arranged is designed as a two-dimensional unit cell. Two transmission poles and one transmission zero are observed with designed unit cell, thus behaving as good isolation between two transmission bands .i.e. C and X-band. The material used is FR-4 with a dielectric constant of 4.3 and a thickness of 0.8 mm. The size of unit cell FSS is $0.40\lambda_0 \times 0.40\lambda_0$ and the thickness of $0.016\lambda_0$, where λ_0 is the first lower resonant frequency. This design is a single layer tri-band frequency selective surface. Two band-pass filters at resonant frequency 6.04 GHz and 9.60 GHz with band-width of 0.89 GHz and 0.87 GHz respectively are obtained. One stop band filter at resonant frequency 7.6 GHz in between C and X-band play an important role in good isolation for wireless communication. Both pass band resonant frequencies are spaced with a good shielding providing the frequency ratio of 1.57. Efficient optimization is done to get both TE and TM polarization.

The design solves the important issues which wireless communication faces. The important points related to the issues encountered in the previous research are focused and the needful solutions done are as follows:

- As per the past researches, the dielectric material and its thickness are present but not shown the effect as an individual, while in this project simulation

related to the variation of dielectric material property and thickness of a substrate keeping unit cell FSS element constant is done and optimized as per desired resonant frequency.

- The complex FSS design is an issue for a conformal airborne platform which is resolved by opting simple design of square slot and cross dipole slot FSS element with FR-4 material of thickness 0.8 mm.

- The effect of insertion of FSS structure in the conformal transmitarray results in the insertion loss which reduces the gain of an antenna which is resolved in this design. The designed FSS has negligible insertion loss with good angular stability and is polarization independent.

- Cylindrical conformal structure of designed unit cell FSS works as an effective band-pass filter for X-band antenna and thus can be an option for real-time radome application with negligible effect on the performance of the antenna.

- In previous research dual-band FSS, resonance frequencies are closely spaced [5], [6], in which proper isolation between the pass-band is the issue, which is resolved in this project.

- A stop-band filter is designed in between the two band-pass filters to get high isolation between the two pass-band for wireless communication applications.

- A simple design is evolved with a single layer providing shielding for C and X bands.

Dielectric Insertion effect on Frequency Selective Surfaces for Band Pass Filter design is analyzed. The effect of various structures like Planar and Conformal along with dielectric, FSS element where gain and insertion loss as a performance factor is observed through simulation for radome application. Apart from this, shielding of the dual band-pass filter is analyzed for wireless application for both TE and TM polarization at various incidence angles. Scattering parameter .i.e. the reflection and transmission parameter of unit cell FSS along with bandwidth is examined. The unit cell FSS is angular stable and polarization independent. The surface current

distribution represents unit cell FSS as a band-pass filter. FSS element and dielectric material are examined through unit cell using floquet boundary analysis method with the help of 3D EM Computational software.

2 RELATED WORK

With the advancement in technology, a lot many Frequency Selective Surface elements are proposed as per the application and frequency band of interest. Many kinds of research and surveys regarding the filters [1],[6],[7],[8],[9],[10],[11], absorbers, and electromagnetic Interference shielding [12], [13] are observed with critical and complex design in military applications and commercial purposes which requires high maintenance. From basic FSS elements like a cross dipole, square loop, patch, circular loop [1], etc., to the complex structure like a square loop with folded arms [8], 3D band-pass FSS design in which substrate is folded several times [10], sandwiched design [11], convoluted meandered [14], flexible serpentine stripe [15], crooked cross geometry convoluted [16] and likewise many more researches are done.

In paper [3] simulation of the whole computer aided design (CAD) model of the stealth bomber B-2 spirit is shown with and without radar absorbing material (RAM) showing the effectiveness of the RAM in the reduction of RCS. Apart from wide-band filter FSS design, research for narrow band-pass FSS is seen in [6] using the coupled method. For wide-band and different band FSS the literature .i.e. [9] find significance by choosing the number of layers. In paper [10], a new design method is proposed in which the thickness of the 3D band-pass FSS is reduced by folding the substrate, thus providing good filtering for conformal structures. Similarly in [5], the 3D FSS are developed from 2D FSS stacked by coupling it using air. Keeping in view the various conformal FSS structures the paper [17] shows the ultra-thin three layer conformal transmit array fed by a horn antenna with various beams of radiation at an oblique incident angle. In the area of development of radome, a new hybrid composite sandwich radome is proposed in [18] showing the stack of layers of various materials .i.e. E-glass/aramid/polyester face sheets with polyvinyl chloride foam are presented which shows the enhancement of the transmission loss in out of band of desired frequency range and good transmission at resonant frequency. In paper [19], the equivalent circuit design method for band-pass FSS and wide-band rejection is proposed, while for high angular stability, the composite sandwich structure is proposed in [20] for radome application. Likewise, by sandwiching a cross dipole

shaped patch slot patch with dielectric, two transmission poles are obtained and are presented in [11]. Similarly to get a low RCS characteristic meta surface is proposed in [21] composed of a metal layer and a dielectric layer.

In the previous studies, the basic linear dipole slots and patches as shown in Fig. 1 are embedded on single layer dielectric substrate are observed in [22] to understand the frequency pulling effect as per the change in thickness of the dielectric material. In paper [23] the dielectric material is proposed which has both FSS characteristics for achieving the resonant frequency and is ultralight mechanical properties by reducing the density of the material. To optimize the resonant frequency and performance, a paper [24] is presented on tunable FSS in which the sliding 3D-printed inserted dielectric is proposed which behaves as a variable capacitance for tuning the resonant frequency. To enhance the gain in patch antenna, ENZ (epsilon near zero) metamaterial superstrate is proposed in [25] to observe the effect of thickness of multi-layer material .i.e. indium antimonide and silicon dioxide. Moving forward for the tri-band pass FSS and miniaturization the paper [14] shows the sandwich dielectric layer between two periodic metallic FSS arrays .i.e. convoluted structure on top and bottom. Same miniaturized 2.5 D FSS is achieved by printing the rectangular spiral FSS elements on both sides of the dielectric are presented in paper [26].

In recent research work, machine learning tools are also used in FSS design like in the synthesis of FSS filters shown in [27] paper for multi-band resonance frequencies. Many designs are proposed to get multi-mode transmission poles and band-reject, out of which recent technology .i.e. 3D structure attracts a lot [28], [29]. PCB with slot lines stacked in normal propagation direction is proposed in [28] to get a multi-mode transmission pole. To meet the real-time scenario both planar and conformal structure is presented with good angular stability in 3D printed and electroplated [29] while the water transfer printed technology is reported in [30]. Many research is observed in the conformal structure transmit array antenna, for various elements like three-layer square ring slots with beam steering [17], hexagonal element [31] while aperture printed on polymide films make it more flexible for any type of conformal structure [32]. Filter enhancement is done by using multiple FSS in a circular cylindrical

structure is presented in [33]. In many research works, the directional radiation is enhanced using the conformal FSS. In paper [34] the hybrid mono-pole dielectric resonator antenna is shown where the FSS radiation enhancement occurs in one band while working as transparent in another band. For good insertion loss based on SIW (substrate integrated waveguide) technique, the ultra-thin planar and conformal structure is proposed in [35]. While in [36] the hybrid structure FSS is used to get ultra-wide stop-band response and the enhanced antenna gain is observed. The antenna performance parameter is observed in [37] that is the gain of the micro strip antenna array. For wide band-pass application, FSS with three layers of FSS element separated by quarter wavelength air gap is proposed in [38]. Various complex and mixed unit cell FSS elements are replicated on planar structure [38] while in paper [39] the two layer huygens element is used for efficient transmitarray applications. Miniaturized dual-band pass FSS at C and X-bands are presented in [40] with meandered monopole aperture element combined with a cross dipole aperture element whereas in [41] the dual-band band-pass FSS is designed through classical theory. In some designs, ultra-wide band-reject filters printed on two different layers of a dielectric substrate with different dielectric constant and thicknesses [42] are observed. By using the coupling effect multi-layer multi-stop band FSS is proposed in [43]. In paper [44] presents 3D FSS by arranging the 2D arrays in a multi-layer fashion to obtain dual-band band-pass filter with an arbitrary band ratio. A Combination of complementary patterns in a compact design is reported in [45] for tri-band characteristics while in [46] for dual-band. Similarly, in [47] dual-band for low frequencies are obtained through two different slot sizes with concentric square patch elements. Tri-band FSS based on various designs like a convoluted, cascaded array of three-square loops with wire grids and square loops with folded arms is proposed respectively in literature [8], [14], [48]. Closely spaced Penta-band FSS is proposed using concentric ring slot resonators in [49]. Likewise, in some unit cell, four apertures are used having tri-band frequencies which are closely spaced with low isolation [50]. In previous research dual-band FSS, resonance frequencies are closely spaced [51], in which proper isolation between the pass-band is the issue, which is resolved in this work.

3 METHODOLOGY

Unit cell FSS is simulated using frequency domain solver of CST software. Floquet boundary analysis is used for obtaining transmission (S21) and reflection (S11) coefficient of FSS.

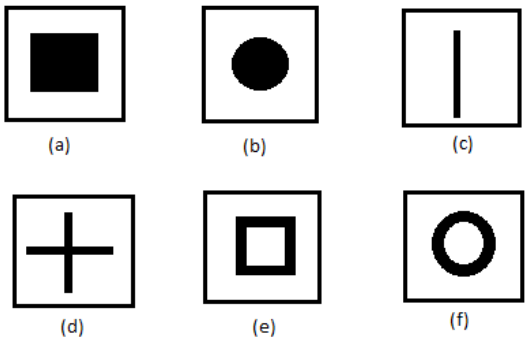

Fig. 1. Various Geometrical Structures of FSS element.

As per the FSS element design, it is a metallic array of patches or slots followed by the thin dielectric as a substrate for providing mechanical strength and maintaining EM transparency. There are various methods to design based on the efficient use of time and cost. Simulation and verification of the designed FSS are done by two methods: Numerical method [5], [10], [14], [25], [26], [52] and Equivalent Circuit Analysis [2], [19], [53], [54], [55], [56]. In this project, various methods like numerical analysis which is a cost effective, showing the exact replica of the prototype and equivalent circuit analysis which is time efficient are used to obtain the Scattering parameter.

As per the unit cell FSS design, it is a metallic patch and slot with a dielectric layer of thickness 0.8 mm of FR-4 material. The dielectric layer which is the substrate of the unit cell FSS element not only provides mechanical strength to the structure but is also used for the optimization of the resonant frequency keeping the FSS element same. FSS element serves as a filter/absorber. Substrate design will have the least effect on the performance of the FSS structure [22] but its property shifts the resonant frequency.

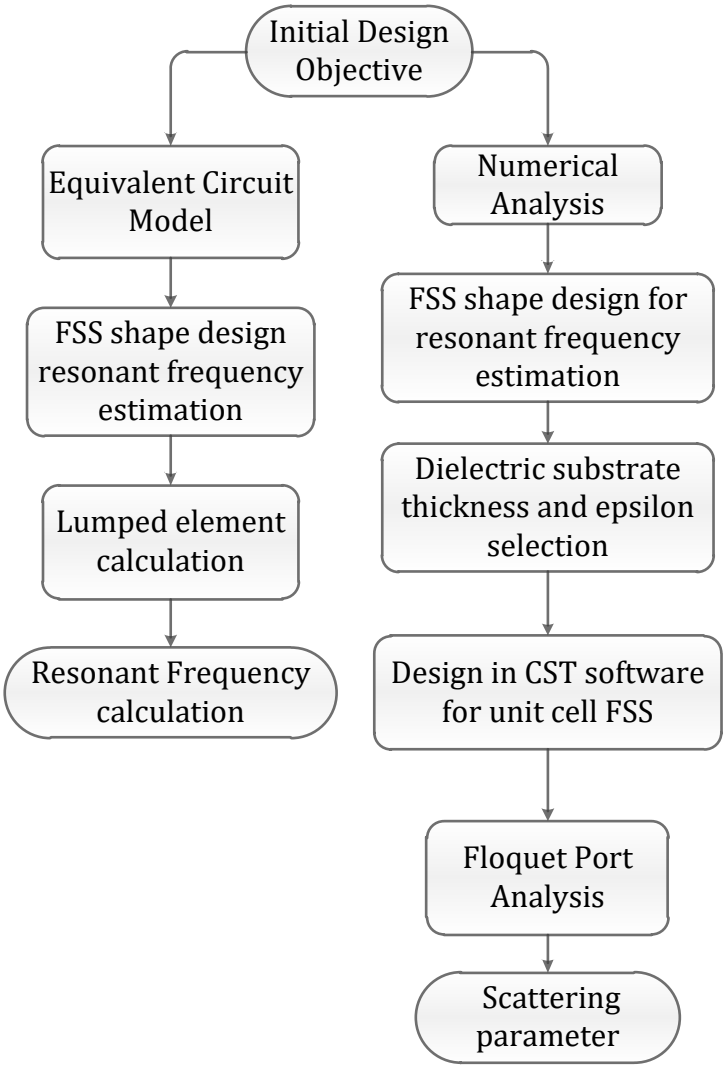

Fig. 2. Flow Chart for the proposed work.

3.1 Equivalent circuit Analysis

There are various methods or techniques for the design and analysis of the FSS structure, one of which is the equivalent circuit model which results in fast prediction of the results [2], [53], [54]. In some papers [2], [53], [54], [55], [56] the FSS behavior is replicated in terms of circuit analysis by showing the design in lumped inductor and capacitors connected in shunt or parallel to get immediate results instead of waiting for full wave simulation results. From paper [57] the equivalent circuit model due to the effect of the shifting of design on double sided FSS is shown. While in paper [52] FSS model is designed using ECM for electromagnetic interference (EMI) shielding application. Initially, an Equivalent circuit model for a single layer is presented

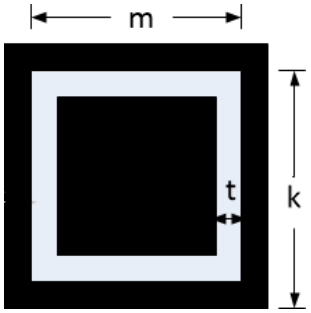

Fig. 3. FSS Structure of Square slot with metallic parts in black colour.

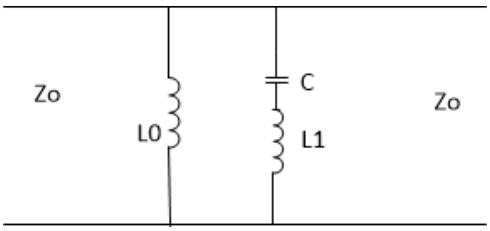

Fig. 4. Equivalent Circuit Model: Square slot shown as shunt LC Circuit.

with the respective equations. FSS layer depicts the filter structure with a parallel connection of inductance and capacitance in a band-pass filter while the dielectric substrate is used as a transmission line response. An Equivalent circuit is the method to analyze FSS and can be seen as an LC circuit, which is based on the shape of the element. For X-band, square slot band-pass filter the equivalent circuit will be a series inductance L1 to capacitor C and is because of the center patch, it is then shunted to an inductance L0.

Equivalent circuit and their respective structures are represented in Fig. 4 and Fig. 3. It suggests the designer adopt the way to meet the required and relevant results. The square slot represents the ECM circuit with a shunt LC for frequency response in the required band. In this square slot, the inner square patch represents the inductance L1 in (3) with a one side length of m-2t. The square inner patch is in series with the capacitance C in (4), while an outer ring of metal which is an inductance L0 in (1) is in shunt with the capacitance, because of the effect of the slot. Thus, the equations are evolved and the equivalent circuit is formed where m,k,t,v are the various parameters of the square slot shown in Fig. 3.

$$\frac{X_{L0}}{Z_0} = \omega L0 = cos\theta F(k, v, \lambda, \theta) \quad \textbf{(1)}$$

$$\frac{X_{L1\text{int}}}{Z_0} = \frac{k-2t}{k} cos\theta F\left(k, m-2t, \lambda, \theta\right) \quad \textbf{(2)}$$

$$\frac{X_{L1}}{Z_0} = \omega L1 = \frac{X_{L1\text{int}}}{Z_0} + \frac{t}{m-2t+v}\frac{X_{L0}}{Z_0} \quad \textbf{(3)}$$

$$\frac{B_C}{Y_0} = 4sec\theta F(k, m, \lambda, \theta) \quad \textbf{(4)}$$

$$F\left(k, \omega, \lambda, \theta\right) = \frac{k}{\lambda}\left[ln\left(cosec\frac{\pi\omega}{2k}\right) + G\left(k, \omega, \lambda, \theta\right)\right] \quad \textbf{(5)}$$

$$G(k, \omega, \lambda, \theta) = \frac{1}{2}\frac{\left(1-\beta^2\right)^2\left[\left(1-\frac{\beta^2}{4}\right)\left(A_+ + A_-\right) + 4\beta^2 A_+ A_-\right]}{\left(1-\frac{\beta^2}{4}\right) + \beta^2\left(1+\frac{\beta^2}{2}-\frac{\beta^4}{8}\right)\left(A_+ + A_-\right) + 2\beta^6 A_+ A_-} \quad \textbf{(6)}$$

$$A\pm = \frac{1}{\sqrt{\left[1\pm\frac{2ksin\theta}{\lambda} - \left(\frac{kcos\theta}{\lambda}\right)^2\right]}} - 1 \quad \textbf{(7)}$$

$$\beta = \left(sin\frac{\pi\omega}{2k}\right) \quad \textbf{(8)}$$

3.2 Numerical Analysis

Numerical analysis frequency response is analyzed through frequency solver as it can sweep to oblique incidence angle while time domain solver can do analysis at normal incidence only. Before moving to prototype fabrication of the design it is efficient to do simulation. Full wave Computer Simulation Software (CST) is used as a 3D EM analysis tool to design FSS. S-parameters and Surface current distribution is obtained through simulation of unit cell FSS using floquet boundary analysis. Fig. 6 shows, the design of the FSS element in CST software while Fig. 5 shows the side view of it. The FSS element is designed based on the circumference of the element which should be effectively one wavelength.

Fig. 5. Geometrical Structure (Side View) with Square slot FSS element and Dielectric Substrate.

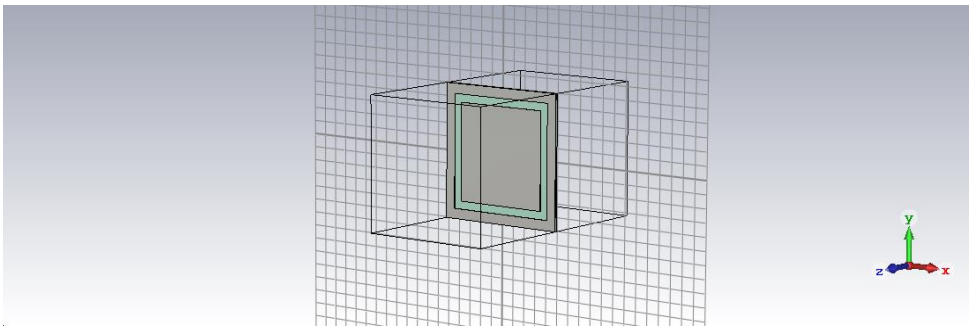

Fig. 6. Geometrical Structure in CST Software with Square slot FSS element and Dielectric Substrate.

In this work first, the regular Square Slot FSS element is designed for X-band that is 8 GHz to 12 GHz frequencies. Unit cell FSS is a single layer with a size of 10mm x 10mm. To stabilize the resonant frequency dielectric substrate is optimized and analyzed to get an efficient frequency response in both TE and TM polarization. The reflection and transmission parameter of frequency along with bandwidth is examined in a unit cell using floquet port analysis.

After final optimization of the substrate, the dielectric layer of thickness 0.8 mm of FR-4 material is used. Further, the unit cell FSS element involved in the design is based on the basic square slot and the cross dipole slot and is replicated in the proposed planar and conformal structure as shown in Fig. 26, Fig. 27 and Fig. 29, Fig. 30 respectively to observe the performance of the antenna through the horn antenna in CST software. Now the excitation is given through plane wave. Stable gain for the antenna is observed after insertion of the planar and conformal FSS structure.

Further, final design of the proposed unit cell FSS is for wireless application. The proposed design consists of two square slots with a concentric square patch and two cross dipole patches arranged diagonally as illustrated in Fig. 32. The size of unit cell FSS is $0.40\lambda_0 \times 0.40\lambda_0$, where λ_0 is the first resonant frequency. The elements involved

in the design are based on the basic square slot with a center square patch and the cross dipole patch FSS element and are combined to form the proposed Unit cell FSS shown in Fig. 32. The unit cell FSS uses floquet boundary analysis to examine the S-parameters and Surface current distribution obtained through simulation results. By making the planar and conformal FSS structure as shown in Fig. 33, the proposed multi-band FSS can be used for wireless applications.

4 SIMULATED RESULTS AND DISCUSSIONS

The parameters to be considered during design are the FSS element size and shape. Apart from the FSS element, substrate plays a vital role in design as it changes the frequency response of FSS. First Influence of the dielectric layer on FSS element is analyzed then the insertion effect of planar, conformal FSS on antenna performance followed by proposed design of dual band-pass and band-stop FSS for wireless communication through CEM software is done. By utilizing the numerical method, accurate data of Scattering parameters that are transmission and reflection coefficients are obtained.

4.1 Dielectric Insertion effect on Frequency Selective Surfaces for Band Pass Filter design

Single layer band-pass FSS results obtained are illustrated from Fig. 7 to Fig. 15 showing the effect of the dielectric material and thickness. These figures present the stability of response with a change in oblique incidence angle for both TE and TM polarization. The dielectric material property is epsilon and thickness is varied and is presented from Fig. 7 to Fig. 14 showing the shift in the resonant frequency. With respect to oblique angle, the resonant nature and bandwidth remain unaffected. The designed FSS are polarization independent.

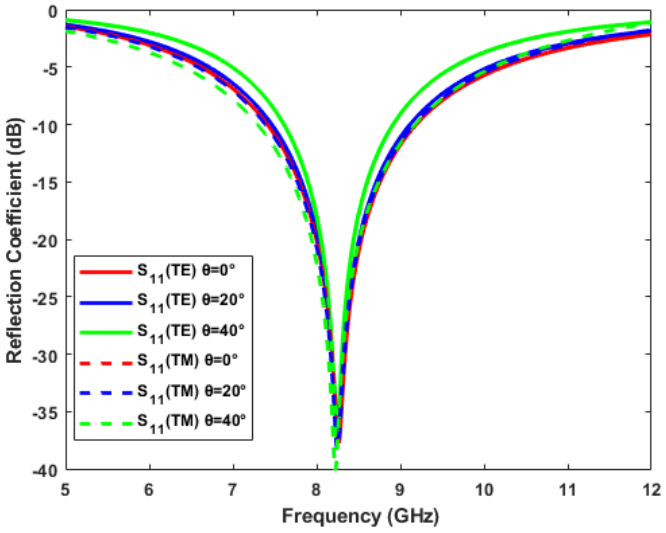

Fig. 7. S-Parameters at Oblique incidence angle, FR-4, thickness=0.50 mm, epsilon=4.3.

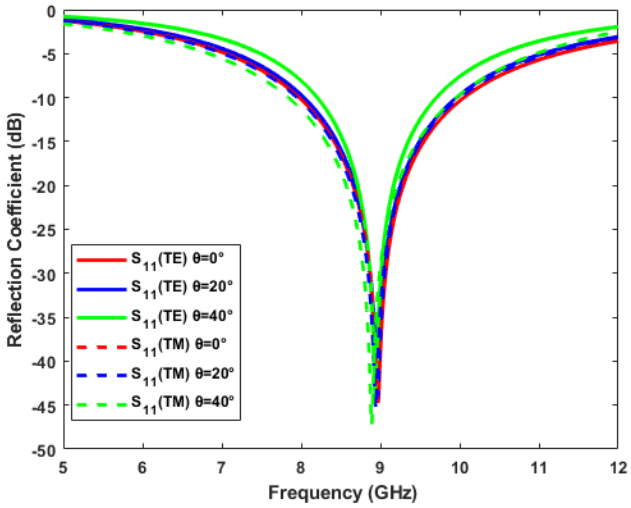

Fig. 8. S-Parameters at Oblique incidence angle, FR-4, thickness=0.30 mm, epsilon=4.3.

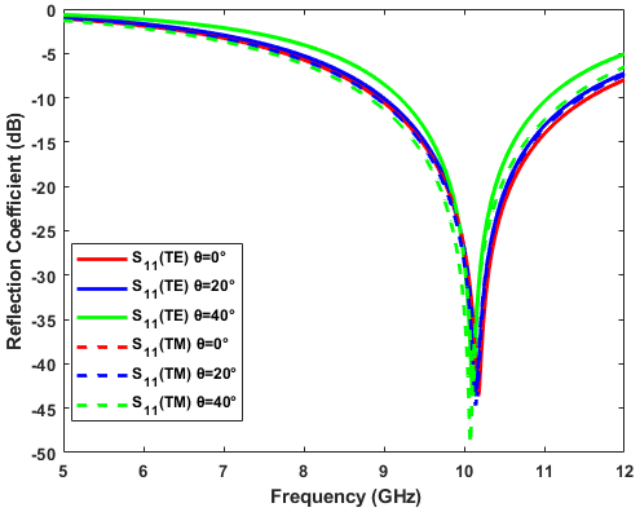

Fig. 9. S-Parameters at Oblique incidence angle, PTFE, thickness=0.50 mm, epsilon=2.1.

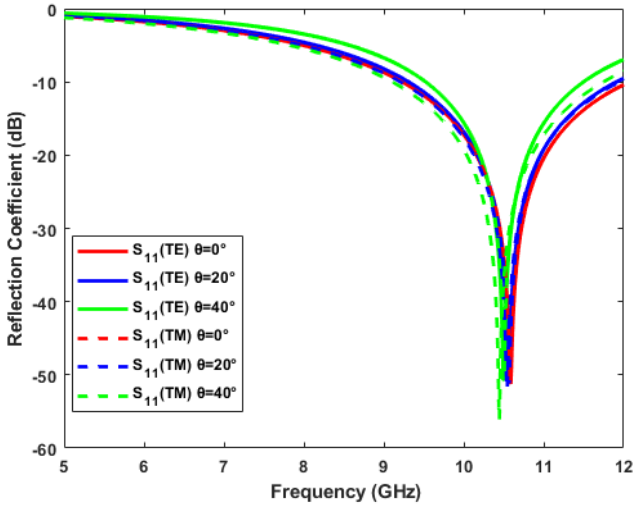

Fig. 10. S-Parameters at Oblique incidence angle, PTFE, thickness=0.30 mm, epsilon=2.1.

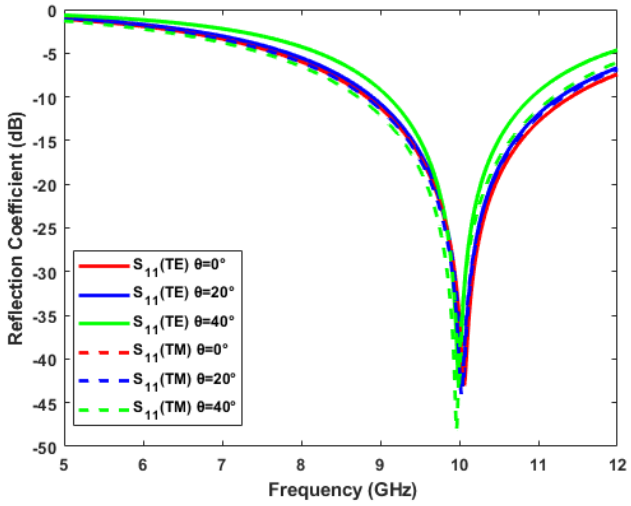

Fig. 11. S-Parameters at Oblique incidence angle, RT5880, thickness=0.50 mm, epsilon=2.0.

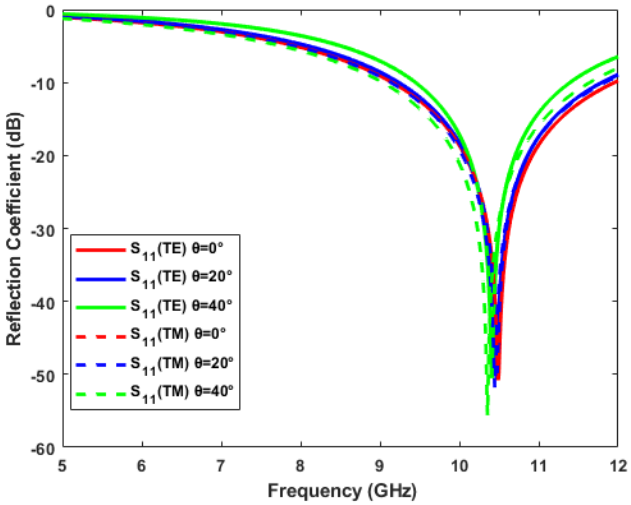

Fig. 12. S-Parameters at Oblique incidence angle, RT5880, thickness=0.30 mm, epsilon=2.0.

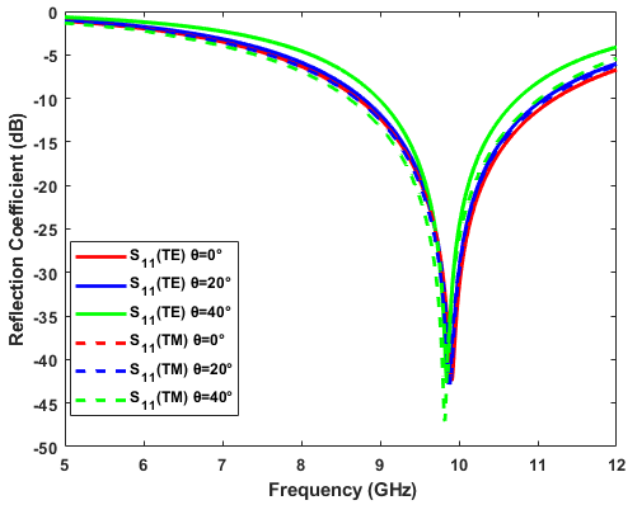

Fig. 13. S-Parameters at Oblique incidence angle, RT5870, thickness=0.50 mm, epsilon=2.33.

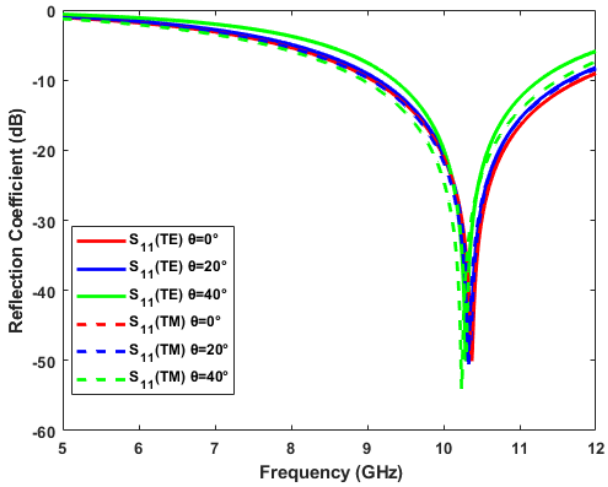

Fig. 14. S-Parameters at Oblique incidence angle, RT5870, thickness=0.30 mm, epsilon=2.33.

As the dielectric constant, that is epsilon decreases towards zero the resonant frequency shifts to a higher frequency and the substrate is behaving like a foam structure. The FR4 substrate of high epsilon corresponds resonant frequency response of 7.9 GHz, while with the same configuration PTFE corresponds to 9.4 GHz and RT5880 to 9.5 GHz.

If consider thickness as a feature in every material, the shift of resonant frequency towards high frequency is observed. As the thickness decrease from 0.50 mm to 0.30 mm FR4 substrate resonant frequency move from 8.26 GHz to 8.96 GHz, PTFE from 10.12 GHz to 10.57 GHz and RT5880 from 10.00 GHz to 10.48 GHz. CEM simulation results are presented in Table I which shows that as the thickness and material properties change, the respective behavioural response to resonant frequency also changes, with a slight change in bandwidth.

There are some limitations to an increase in the thickness of the dielectric. As the thickness of the dielectric increase beyond $\lambda/10$, the losses are introduced which are easily visible through the transmission and reflection coefficient plot obtained which is shown in Fig. 15. Dielectric thickness of 3 mm with the same unit cell FSS design does not show any transmission at the desired resonant frequency and the insertion loss is too high with high return loss.

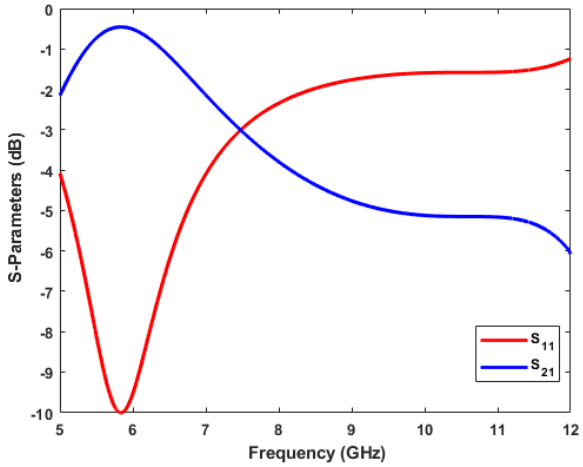

Fig. 15. S-Parameters at Normal incidence angle, FR4, thickness=3.0 mm, epsilon=4.3.

TABLE-I

ANALYSIS OF INFLUENCE OF DIELECTRIC MATERIAL AND THICKNESS FOR BOTH TE AND TM POLARIZATION

Material	Thickness(mm)	Dielectric Constant (epsilon)	Resonant Frequency (GHz)
FR4	0.50	4.3	8.26
FR4	0.30	4.3	8.96
PTFE	0.50	2.1	10.12
PTFE	0.30	2.1	10.57
RT5880	0.50	2.0	10.00
RT5880	0.30	2.0	10.48
RT5870	0.50	2.33	9.90
RT5870	0.30	2.33	10.33

4.2 Stable Gain With Frequency Selective Surface in Planar and Conformal Structure: For Radome Application

After the study and simulation of the dielectric material as an individual effecting the design, the combined effect of the FSS element and dielectric layer are examined by frequency domain solver in CST software. The unit cell FSS uses floquet boundary analysis to examine the S-parameters and surface current distribution obtained through simulation. After final optimization of the substrate, the dielectric layer of thickness 0.8 mm of FR-4 material is used. The size of unit cell FSS is $0.32\lambda_0 \times 0.32\lambda_0$, where λ_0 is the resonant frequency. Further, the unit cell FSS element involved in the design is based on the basic square slot and the cross dipole slot and is replicated in the proposed planar and conformal structure as shown in Fig. 26, Fig. 27 and Fig. 29,

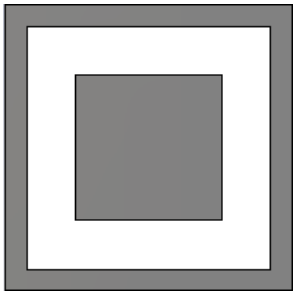

Fig. 16. Square Slot with center square patch Unit cell FSS (10 × 10 mm) with metallic part in grey colour.

Fig. 30 respectively to observe the performance of the antenna through the horn antenna in CST software. Now the excitation is given through plane wave. Stable gain for the antenna is observed after insertion of the planar and conformal FSS structure. As per the square slot and the cross dipole slot unit cell FSS design, the metallic part of the FSS element is shown in grey color in Fig. 16 and Fig. 17 with a dielectric layer of thickness 0.8 mm of FR-4 material.

Both square slot and cross dipole slot are polarization independent presented in Fig. 18 and Fig. 22 for the respective unit cell FSS and show excellent angular stability. Reflection and Transmission Coefficients are shown in Fig. 19, Fig. 20 and Fig. 23, Fig. 24 respectively for square slot and cross dipole slot unit cell FSS. The surface current distribution is presented in Fig. 21 and Fig. 25 for the square slot and cross dipole slot respectively. The surface current distribution plot obtained shows the current flow in the various branches of the FSS element resonating at 9.6 GHz and 9.57 GHz for square slot and cross dipole slot respectively.

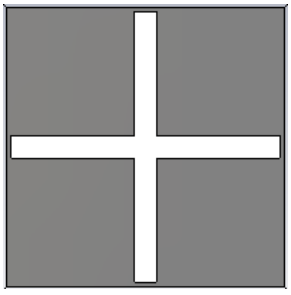

Fig. 17. Cross Dipole Slot FSS Element (10 × 10 mm) with metallic parts in grey colour.

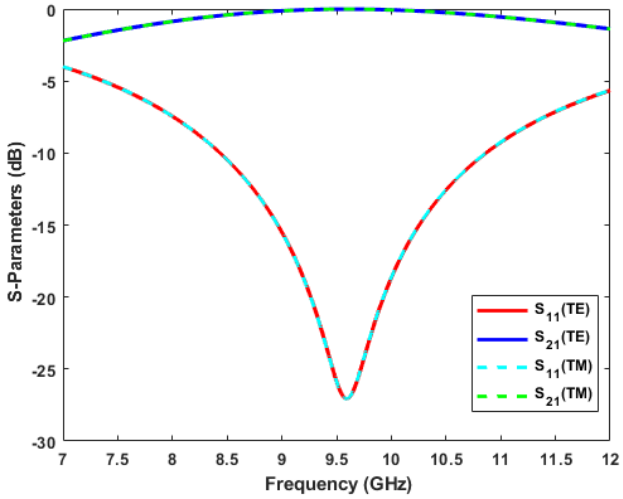

Fig. 18. S-parameter for Square Slot FSS for TE and TM polarization at normal incidence angle.

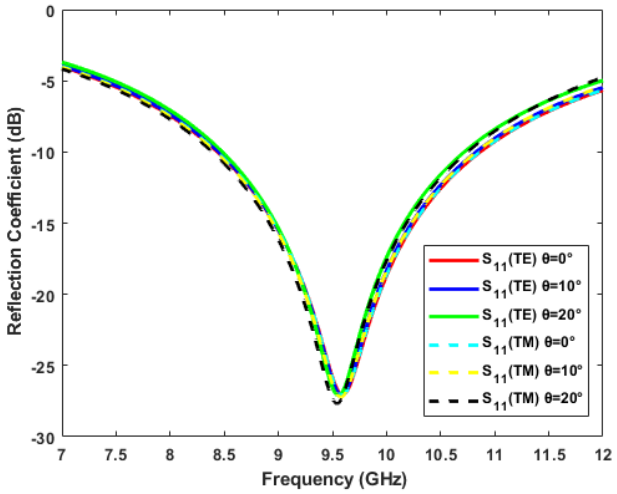

Fig. 19. Reflection Coefficient for Square Slot FSS element for both TE and TM at oblique incident angle.

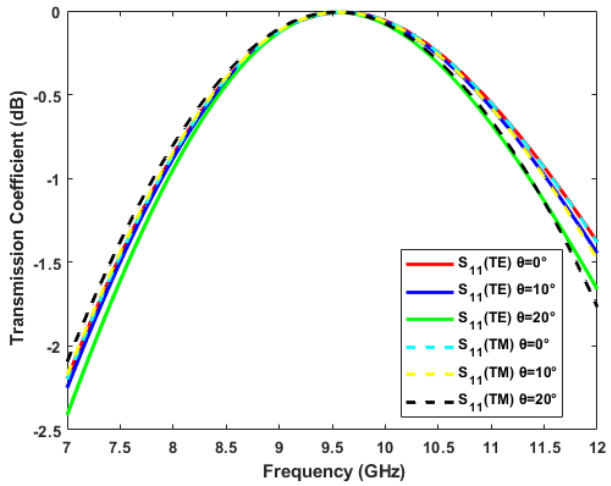

Fig. 20. Transmission Coefficient for Square Slot FSS element at Oblique incident for TE and TM polarization

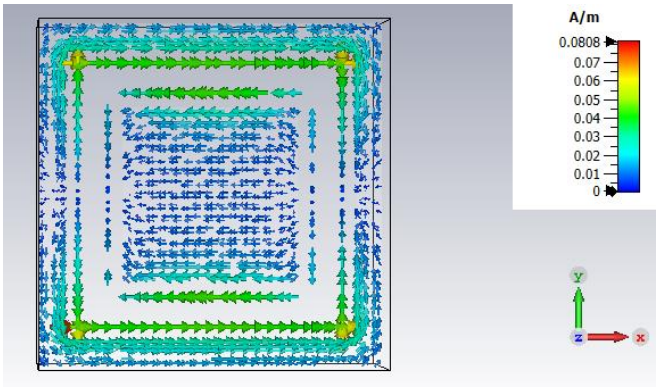

Fig. 21. Surface current distribution of Square Slot FSS element.

Fig. 19 and Fig. 20 show the reflection and transmission coefficient for square slot FSS elements while Fig. 23 and Fig. 24 show the reflection coefficient (s11) and transmission coefficient (s21) for cross dipole slot. The s-parameters at normal incidence for both TE and TM polarization are presented in Fig. 18 and Fig. 22 for square slot and cross dipole slot FSS respectively.

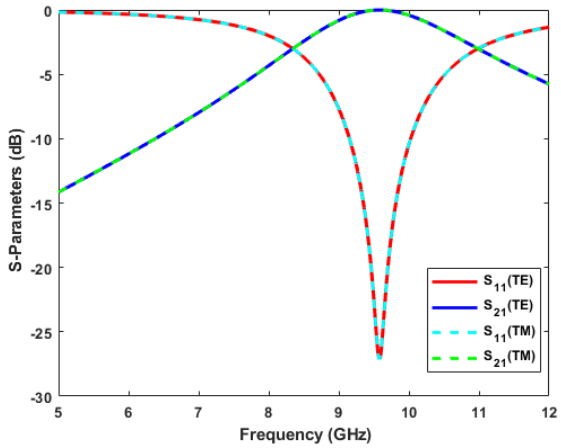

Fig. 22. S-parameter for Cross Dipole Slot FSS for TE and TM polarization at normal incidence angle.

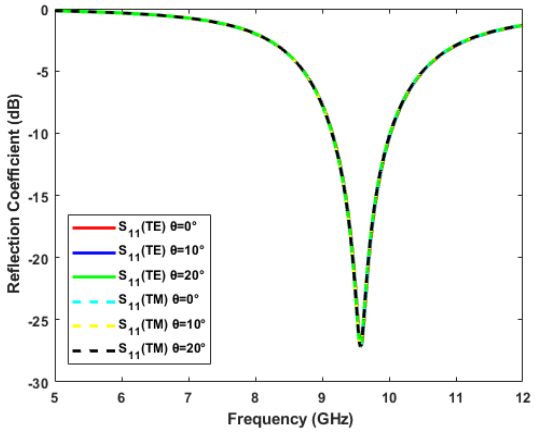

Fig. 23. Reflection Coefficient for Cross Dipole Slot FSS for both TE and TM at oblique incident angle.

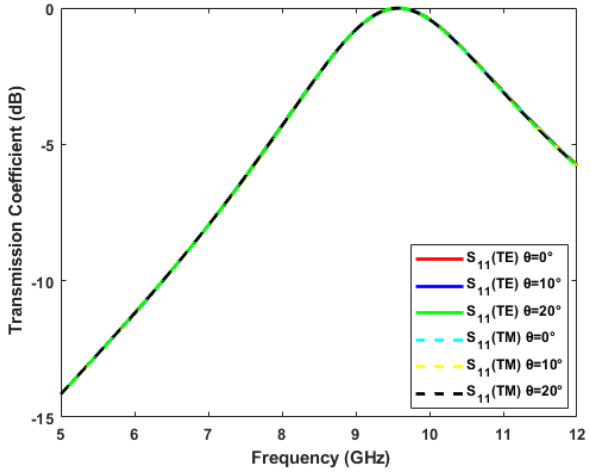

Fig. 24. Transmission Coefficient for Cross Dipole Slot FSS at Oblique incident for TE and TM polarization.

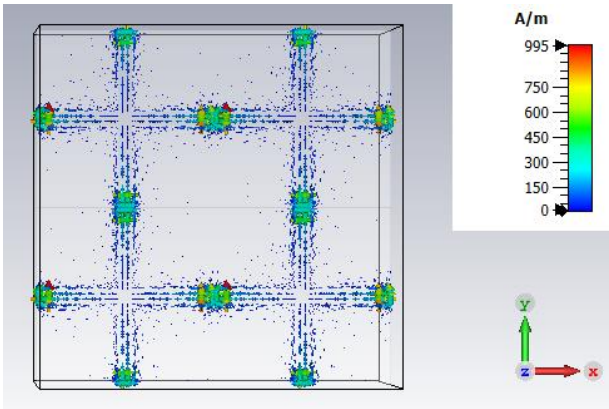

Fig. 25. Surface current distribution of Cross Dipole Slot FSS element

Insertion loss along with gain enhancement is observed through the gain factor in the frequency band of interest. The resonant frequency obtained by tuning is 9.6 GHz and 9.57 GHz respectively for the square slot and cross dipole slot FSS element. The band-width observed is 2.38 GHz and 0.86 GHz at -10 dB insertion loss for both square slot and cross dipole slot respectively.

For the evaluation of the performance parameter of the FSS element, it is replicated from the unit cell to the planar and conformal FSS structure and is simulated using the horn antenna. Simulated results with and without antenna are illustrated in Fig. 28 and Fig. 31. A Summary of the s-parameters results of unit cell FSS is shown in Table II. Planar and Conformal are simulated with an antenna and the performance is shown in Table III.

TABLE II

S-PARAMETER RESULTS OF THE UNIT CELL FSS USING FLOQUET BOUNDARY ANALYSIS

FSS Element	Reflection Coefficient S11 (dB)	Transmission Coefficient S21 (dB)	Bandwidth@- 10dB
Square Slot	−27.06	−0.0085	2.38 Ghz
Cross Dipole Slot	−27.14	−0.0088	0.86 Ghz

The structure involved in the design is based on the basic square slot and the cross dipole slot FSS element and is replicated in the proposed planar and conformal structure as shown in Fig. 26, 27, 29 and Fig. 30. Stable gain with enhancement is observed in table form for planar and conformal FSS structure.

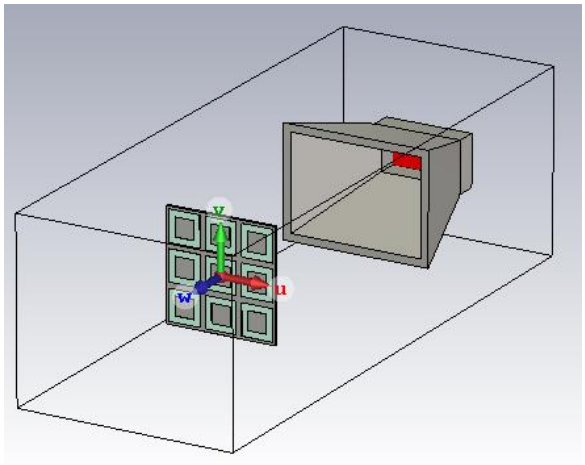

Fig. 26. Horn antenna with Planar Square Slot FSS element structure in CST software

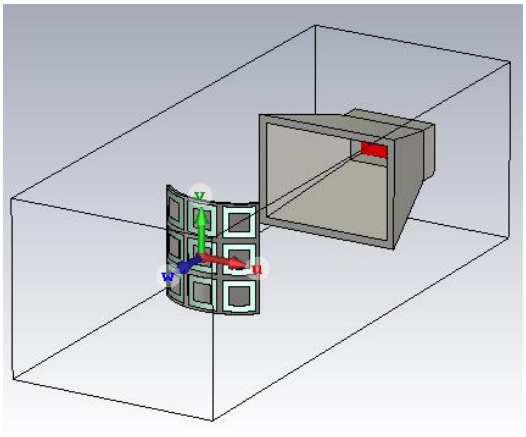

Fig. 27. Horn antenna with Conformal Square Slot FSS element structure in CST software

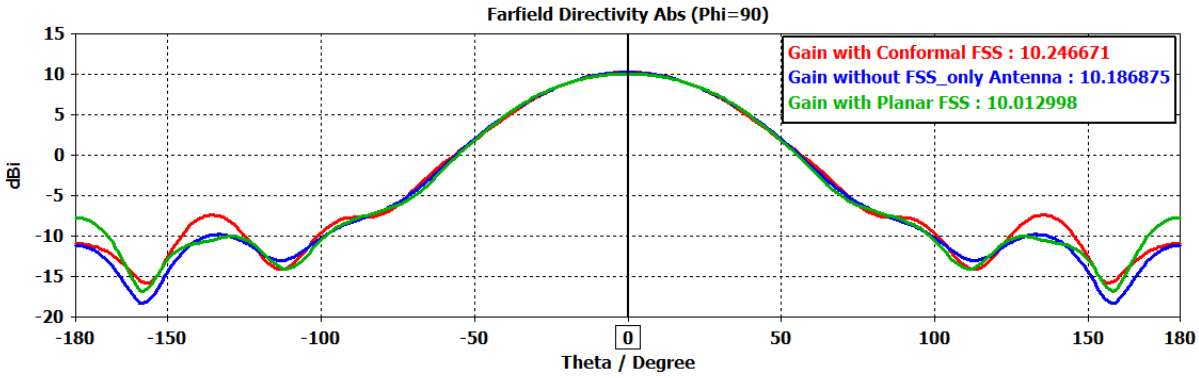

Fig. 28. Gain (dBi) vs Theta (degree) with and without FSS for Square Slot element structure

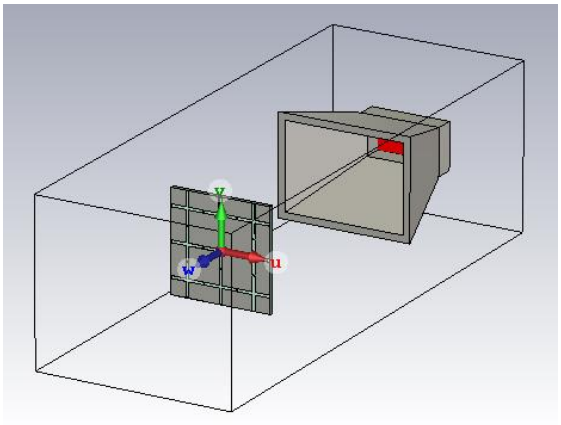

Fig. 29. Horn antenna with Planar Cross Dipole Slot FSS element structure in CST software

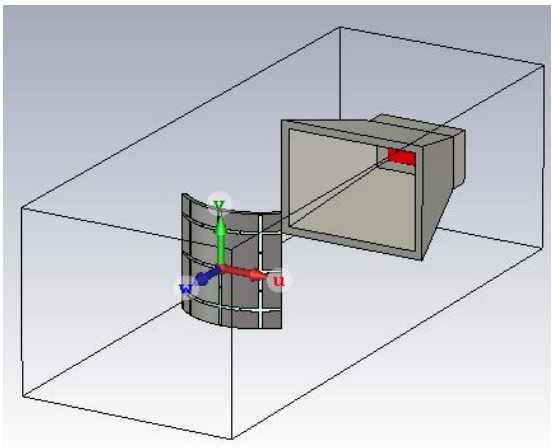

Fig. 30. Horn antenna with Conformal Cross Dipole Slot FSS element structure in CST software

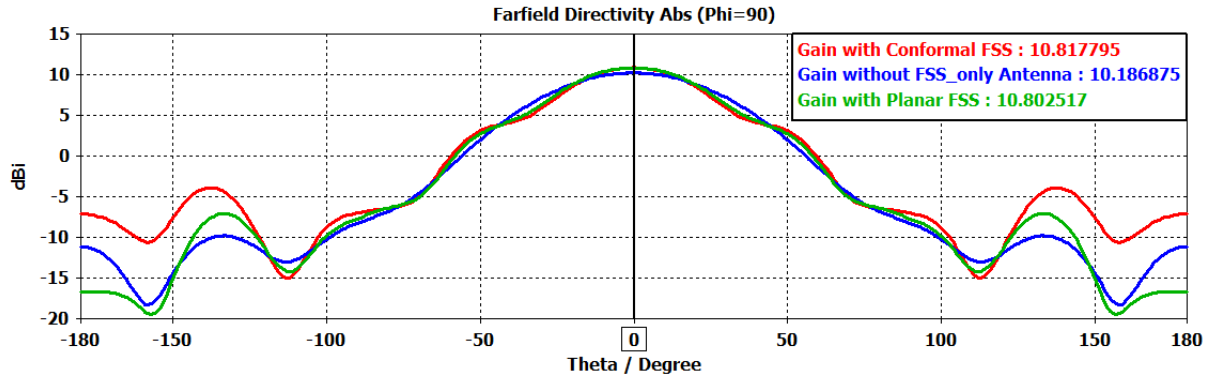

Fig. 31. Gain (dBi) vs Theta (degree) with and without FSS for Cross Dipole Slot element structure

Two simulations are done one with FSS and the other without FSS and the results are compared. Compared results and the influence of the FSS structure are presented in Table III. From the results obtained it is analyzed that the gain as a performance parameter is more or less similar when using FSS as a band-pass filter for planar and conformal structure. A comparison with the existing research is shown in Table IV.

TABLE III

RESULTS OBTAINED DUE TO THE INFLUENCE OF FSS STRUCTURE (PLANAR AND CONFORMAL) WITH ANTENNA TAKING GAIN AS PERFORMANCE PARAMETER

FSS Element	FSS Structure	Gain of Antenna Without FSS (dB)	Gain of Antenna with FSS (dB)	10 dB relative BW (%)	Insertion Gain or Loss (dB)
Square Slot	Planar	10.1868	10.0129	2.38	0.17 loss
	Conformal	10.1868	10.2466	2.38	0.06 gain
Cross Dipole Slot	Planar	10.1868	10.8025	0.86	0.62 gain
	Conformal	10.1868	10.8177	0.86	0.63 gain

TABLE IV

COMPARASION WITH THE EXISTING RESULTS

Ref.	Fabrication Complexity of design Element	Unit cell Size	Thickness	Substrate Epsilon	Resonant frequency	Insertion Gain or Loss(dB)
[17]	3D FSS complex (mix of square slot)	$0.46\lambda_0 \times 0.46\lambda_0$	$0.04\lambda_0$ (stack of substrate)	2.2	25	3.8 loss
[35]	Y shaped slot	$0.56\lambda_0 \times 0.56\lambda_0$	$0.055\lambda_0$	2.2	11.2, 11.43	0.3 loss
[39]	huygens	$0.28\lambda_0 \times 0.28\lambda_0$	$0.016\lambda_0$	3.55	10	1.67 loss
This Paper	Simple Square Slot	$0.333\lambda_0 \times 0.333\lambda_0$	$0.026\lambda_0$	4.3	9.6	0.06 gain
This Paper	Simple Cross Dipole Slot	$0.319\lambda_0 \times 0.319\lambda_0$	$0.025\lambda_0$	4.3	9.57	0.63 gain

4.3 Design of Dual Band Pass and Band Stop Frequency Selective Surface: For Wireless Communication

Finally, both unit cell FSS are further used for the final design of the proposed tri-band unit cell FSS for wireless application. The proposed design consists of two square slots with a concentric square patch and two cross dipole patches arranged diagonally as illustrated in Fig. 32. The size of unit cell FSS is $0.40\lambda_0 \times 0.40\lambda_0$, where λ_0 is the first resonant frequency. The structure involved in the design is based on the basic square slot with a center square patch and the cross dipole patch FSS element and is combined to form the proposed Unit cell FSS shown in Fig. 32. By making the planar and conformal FSS structure as shown in Fig. 33, the proposed multi-band FSS can be used for wireless applications.

The single layer Unit cell FSS is simulated in frequency domain solver using floquet boundary condition to obtain S-parameters. Influence of two different simple FSS

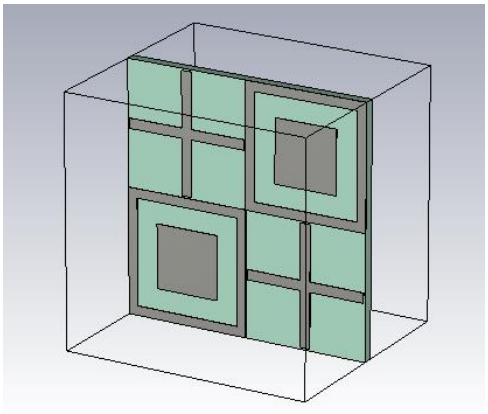

Fig. 32. Unit cell FSS element in CST Software.

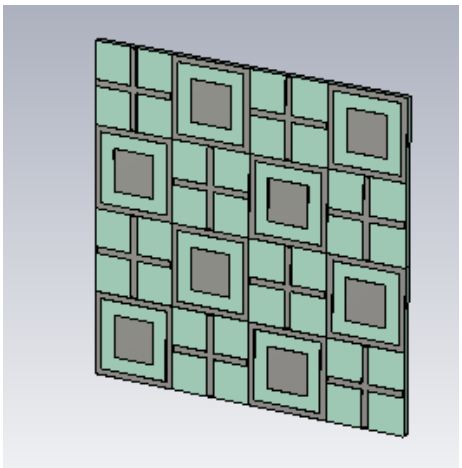

Fig. 33. Planar FSS structure of designed unit cell in CST Software.

elements are analyzed through CEM software. By utilizing the numerical methods, accurate data of scattering parameters that is transmission and reflection coefficients are obtained shown in Fig. 34. Fig. 34 depicts the transmission and reflection coefficient in TE and TM polarization at a normal incident angle showing stability at the resonant frequencies. As per Fig. 34 two resonance transmission poles .i.e. at 6.04 GHz and 9.60 GHz are obtained with a loss of 0.0013 and 0.0084 respectively. The two pass-band characteristics at 6.04 GHz and 9.60 GHz are achieved with a band-width of 0.89 GHz and 0.87 GHz respectively at -10dB insertion loss. The frequency ratio obtained through this pass-band is 1.57. Apart from this dual pass-band, one band-stop in between this dual pass-band is obtained with a resonant frequency of 7.6 GHz and band-width of 0.67 GHz which work as shielding for these two pass-bands.

Phase characteristics are also presented for transmission and reflection coefficients in Fig. 35. From Fig. 35 it is evident that the phase of reflection coefficient at 6.04 GHz and 9.60 GHz is zero thus it behaves as a ground plane for antenna at respective frequencies which act as FSS ground and hence contribute to the increase of gain at resonant frequencies of the pass-band. Fig. 36 and Fig. 37 shows the reflection and transmission coefficient respectively at various incident angle for both TE and TM polarization which shows the stability of the resonant frequency in C-band while a slight shift in X-band. The design results with an insertion loss of 0.0013 and 0.0084 at two pass-band transmission poles are obtained.

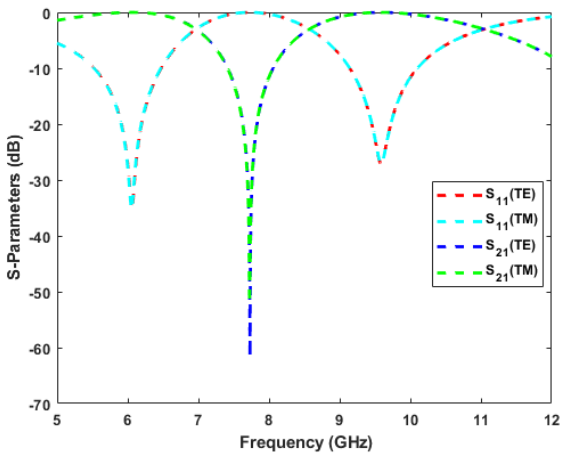

Fig. 34. Simulated S-Parameters at Normal incidence angle for both TE and TM polarization

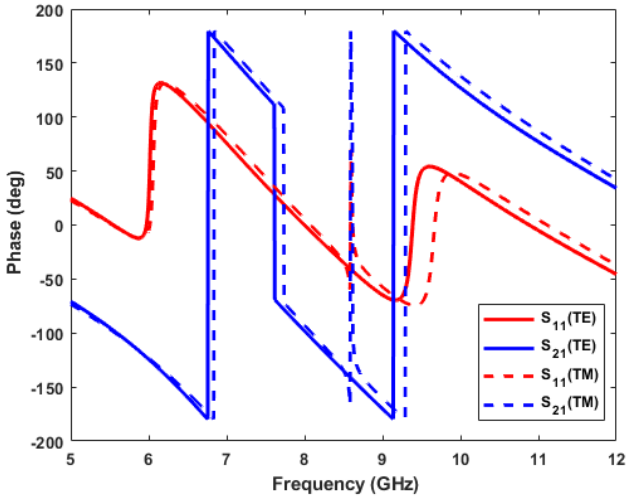

Fig. 35. Simulated Phase response of Transmission and Reflection Coefficient at normal incidence angle for both TE and TM polarization

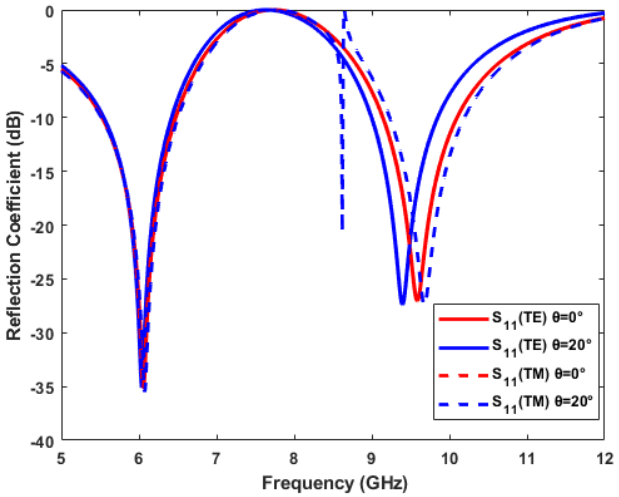

Fig. 36. Simulated Reflection Coefficient at various incidence angle for both TE and TM polarization.

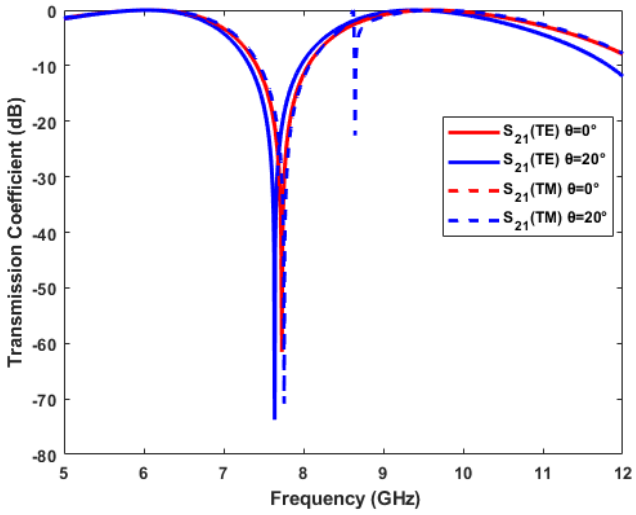

Fig. 37. Simulated Transmission Coefficient at various incidence angle for both TE and TM polarization

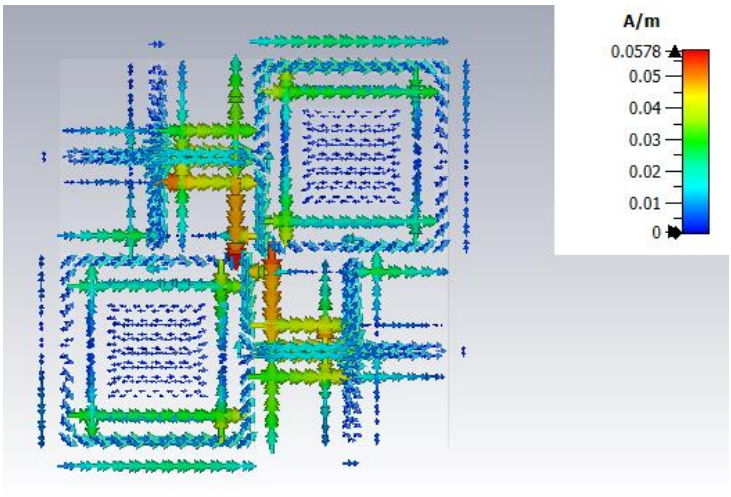

Fig. 38. Surface current distribution at 6.04 GHz.

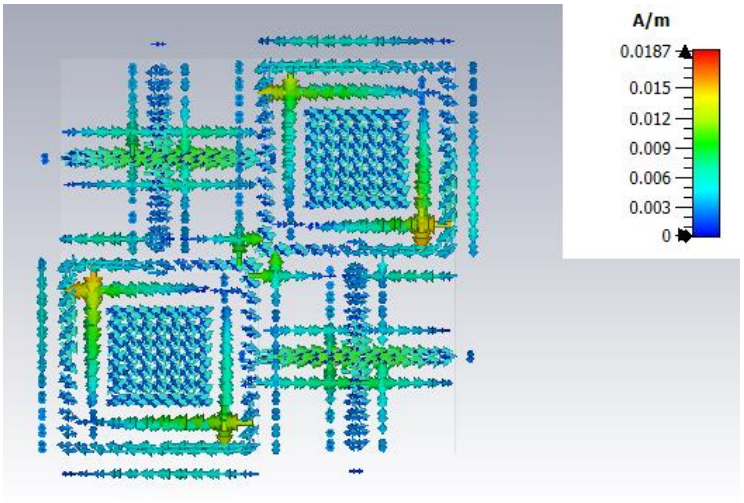

Fig. 39. Surface current distribution at 9.60 GHz.

The surface current distribution of the unit cell FSS is investigated in this thesis. As per the surface, the current distribution plot obtained in the simulation is shown in Fig. 38 and Fig. 39 which indicates the current flow direction in the various arms of the FSS element. In Fig. 38 the surface current concentration is seen at various branches of the unit cell resonators for resonant frequency 6.04 GHz while Fig. 39 represents the resonant frequency at 9.60 GHz.

The CEM results are depicted in the table form. Table V shows the summary of the results obtained. Comparative analysis with the previous work done in research with this work is shown in Table VI.

TABLE V

SUMMARY OF SIMULATED S-PARAMETERS AT NORMAL INCIDENCE ANGLE

Band	Resonant Frequency (GHz)	Band Ratio	S11 (dB)	Loss (dB) at transmission zero	Bandwidth @ -10dB
C	6.04	1.57	−35.21	−0.0013	0.89 Ghz
X	9.60	1.57	−27.09	−0.0084	0.87 Ghz

TABLE VI

COMPARATIVE ANALYSIS WITH THE EXISTING RESEARCH PAPERS

Ref	Resonant Frequency (GHz)	Unit cell Size	Thick-ness	No. of Layer	Frequency Ratio	Dielectric constant (ϵ)	Band width (GHz)
[13]	2.40, 5.00	$0.076\lambda_0 \times 0.076\lambda_0$	$0.012\lambda_0$	1	2.08	2.65	0.23, 0.30@ −20dB
[16]	2.54, 3.54	$0.088\lambda_0 \times 0.088\lambda_0$	$0.013\lambda_0$	1	1.39	4.3	0.315, 0.178@ − 15dB
[46]	2.4, 5.2	$0.086\lambda_0 \times 0.086\lambda_0$	$0.008\lambda_0$	1	2.17	4.4	1.75, 2.20@ − 10dB
[47]	1.73, 2.64	$0.115\lambda_0 \times 0.115\lambda_0$	$0.058\lambda_0$	1	1.53	2.65	0.31, 0.26@ − 1dB
[50]	8.1, 9.8, 11	$0.55\lambda_0 \times 0.55\lambda_0$	$0.022\lambda_0$	1	1.2, 1.12	3.38	_
This Paper	6.04, 9.60	$0.40\lambda_0 \times 0.40\lambda_0$	$0.016\lambda_0$	1	1.57	4.3	0.89, 0.87@ − 10dB

5 CONCLUSION

In this project FSS element and dielectric material are examined through frequency domain solver using floquet boundary analysis method with the help of 3D EM Computational software. Various analysis are done step by step for FSS based Band Pass Filter design. Firstly Dielectric Insertion effect on Frequency Selective Surfaces for Band Pass Filter design is analyzed, then the effect of various structures like Planar and Conformal with dielectric as a substrate is observed, where gain and insertion loss as a performance factor is observed through simulation for radome application. Apart from this finally, the design of dual band-pass and band-stop FSS providing shielding for the filter is analyzed for wireless application for both TE and TM polarization at various incidence angles. Thus, tri-band frequency selective surfaces are designed that is two transmission poles and one transmission zero to obtain good isolation between C and X-band for wireless communication.

Scattering parameter .i.e. the reflection and transmission parameter of unit cell FSS along with bandwidth is examined. The unit cell FSS is angular stable and polarization independent. The surface current distribution represents unit cell FSS as a band-pass filter.

It is found through the results that apart from the FSS element shape, the dielectric layer thickness and material provide aid for tuning the resonant frequency. EM simulation is carried out and the results presented the stable response with a change in oblique incidence angle which analyse that the shift in resonant frequency is not only due to FSS element shape but also due to the dielectric thickness and material property. There are some limitations to an increase in the thickness of the dielectric. As the thickness of the dielectric increases beyond $\lambda/10$, the losses are introduced which are easily visible through the scattering parameter. Dielectric thickness of 3 mm with the same unit cell FSS design is not showing any transmission at the desired resonant frequency and the Insertion loss is too high with high return loss.

Afterward, the simple FSS element that is a square slot and cross dipole slot is designed as a filter and simulated on conformal structure form for airborne platform

application with negligible insertion loss. The reflection and transmission coefficients are the characteristics of the designed filter which shows significant band-width in both C and X-Band at -10 dB insertion loss. Some insertion loss of antenna for a conformal airborne platform is resolved in this work by opting simple design by maintaining the stable gain of the antenna as a performance parameter of FSS. Good angular stability is observed for both square slot and cross dipole slot. Performance of antenna with FSS and without FSS in planar and conformal structure is observed by simulating through horn antenna. Thus, summarizes the performances of the two different FSS elements in X-Band in terms of s-parameters, gain and band-width while the results show the influence of the planar and conformal FSS on antenna performance. It is concluded that conformal structure gives gain enhancement more than the planar while cross slot shows enhanced gain with respect to the square slot. This work highlights the possibility to use a simple FSS element by presenting a good performance of FSS in terms of the gain of an antenna. Therefore, a simple FSS element can be used as an option for real-time application use with no effect on the performance of the antenna when FSS is used and on the other hand achieves RCS reduction.

While for wireless communication, both unit cell FSS are further used for the final design of the proposed tri-band frequency selective surface .i.e. two transmission poles and one transmission zero. It is concluded by showing the dual band-pass FSS resonating at 6.04 GHz and 9.60 GHz isolated with stop-band FSS at 7.6 GHz resonating frequency presenting the performance parameter in terms of band ratio, reflection coefficient, loss and bandwidth. This provides good isolation between the two pass-band FSS at C and X-band. With low FSS thickness .i.e. 0.8 mm a good frequency ratio that is 1.57 is obtained. It is concluded that a combination of two basic FSS elements results in the dual band-pass FSS with good isolation and can be used in the field of wireless communication.

While for further future work, optimization on the same final designed unit cell FSS element can be used to simulate complete radome structure to see the feasibility and effect on the performance of the antenna.

REFERENCES

[1] B. A. Munk. Frequency Selective Surfaces: Theory and Design. Hoboken, NJ, USA: Wiley, ISBN 0-471-37047-9, 2000.

[2] F. Costa, A. Monorchio, G. Manara,“ An Overview of Equivalent Circuit Modeling Techniques of Frequency Selective Surfaces and Metasurfaces," Applied Computational Electromagnetics Society Journal, 29(12), 2014.

[3] M. A. Alves, R. J. Port and M. C. Rezende,“ Simulations of the radar cross section of a stealth aircraft," SBMO/IEEE MTT-S International Microwave and Optoelectronics Conference, 409-412, 2007.

[4] V. A. Vincent, C. Kailasanathan, G. Ramesh et al,“ Fabrication and Characterization of Hybrid Natural Fibre-Reinforced Sandwich Composite Radar Wave Absorbing Structure for Stealth Radomes," Transactions on Electrical and Electronic Materials, 22, 794–802, 2021.

[5] A. K. Rashid, B. Li, Z. Shen,“ An overview of three-dimensional frequency-selective structures,” IEEE Antennas and Propagation Magazine, 56(3), 43–67, 2014.

[6] H. H. Chou, G. J. Ke,“ Narrow Bandpass Frequency Selective Surface With High Level of Angular Stability at Ka-Band,” in IEEE Microwave and Wireless Components Letters, 31(4), 361-364, April 2021.

[7] R. S. Anwar, Y. Wei, L. Mao and H. Ning,“ Miniaturised frequency selective surface based on fractal arrays with square slots for enhanced bandwidth,” IET Microwaves, Antennas Propagation, 13(11), 1811- 1819(8), 2019.

[8] M. Bashiri, C. Ghobadi, J. Nourinia and M. Majidzadeh,“ WiMAX, WLAN, and X-Band Filtering Mechanism: Simple-Structured Triple-Band Frequency Selective Surface,” in IEEE Antennas and Wireless Propagation Letters, 16, 3245-3248, 2017.

[9] K. Sarabandi and N. Behdad,“ A Frequency Selective Surface With Miniaturized Elements,” in IEEE Transactions on Antennas and Propagation, 55(5), 1239-1245, May 2007.

[10] A. A. Omar and Z. Shen,“ Thin 3-D Bandpass Frequency-Selective Structure Based on Folded Substrate for Conformal Radome Applications," in IEEE Transactions on Antennas and Propagation, 67(1), 282-290, Jan. 2019.

[11] R. Ratnam, A. Hemasree, S. Mahato, S. Kundu and A. Chatterjee,“ A Cross-Dipole Shaped Patch-Slot-Patch Bandpass Frequency Selective Surface,” IEEE URSI Regional Conference on Radio Science (URSIR-CRS), 1–3, 2020.

[12] M. Yan et al.,“ A miniaturized dual-band FSS with stable resonance frequencies of 2.4 GHz/5 GHz for WLAN applications,” IEEE Antennas Wireless Propag. Lett., 13, 895–898, May 2014.

[13] K. Sangeethalakshmi, S. Rukmani Devi, N. Gangatharan, P. Sivalakshmi,“ Challenges opportunities in frequency selective surfaces for EMI shielding application: A theoretical survey,” Materials Today: Proceedings, 43(6), 3947-3950, 2021.

[14] N. Liu, X. Sheng, C. Zhang, J. Fan, D. Guo,“ A Miniaturized Triband Frequency Selective Surface Based on Convoluted Design,” IEEE Antennas and Wireless Propagation Letters, 16, 2384-2387, 2017.

[15] S. Chen et al.,“ Flexible Serpentinelike Frequency Selective Surface for Conformal Applications With Stable Frequency Response,” in IEEE Antennas and Wireless Propagation Letters, 18(7), 1477-1481, July 2019.

[16] R. Sivasamy and M. Kanagasabai,“ A novel dual-band angular independent FSS with closely spaced frequency response,” IEEE Microw. Wireless Compon. Lett., 25(5), 298–300, May 2015.

[17] P. Y. Qin, L. z. Song and Y. J. Guo,“ Beam Steering Conformal Transmitarray Employing Ultra-Thin Triple-Layer Slot Elements,” in IEEE Transactions on Antennas and Propagation, 67(8), 5390-5398, Aug. 2019.

[18] H. Rafieipour, A. Setoodeh, A. K. T. Lau,“ Mechanical and electromagnetic behavior of fabricated hybrid composite sandwich radome with a new optimized frequency-selective surface,” Composite Structures, 273, 114256, 2021.

[19] N. Liu, X. Sheng, C. Zhang and D. Guo,“ Design and Synthesis of Band-Pass Frequency Selective Surface With Wideband Rejection and Fast Roll-Off Characteristics for Radome Applications,” in IEEE Transactions on Antennas and Propagation, 68(4), 2975-2983, April 2020.

[20] N. Liu, X. Sheng, C. Zhang and D. Guo,“ Design of Frequency Selective Surface Structure With High Angular Stability for Radome Application,” in IEEE Antennas and Wireless Propagation Letters, 17(1), 138-141, Jan. 2018.

[21] Z. Zhang, X. Cao, H. Yang, T. Li, J. Tian, and J. Gao,“ Novel strategy to design a metasurface with integrated radiation and a broadband low radar cross section,” Optical Material Express, 11(11), 3636-3645, 2021.

[22] P. Callaghan, E.A. Parker, R.J. Langley,“ Influence of supporting dielectric layers on the transmission properties of frequency selective surfaces,” IEE Proceedings H Microwaves, Antennas and Propagation, 138(5), 448–454, 1991.

[23] L. Li, W. Jiang, J. Wang, H. Ma, and S. Qu,“ Feasible strategy for simultaneously achieving excellent frequency selective characteristic and ultralight mechanical properties,” Optics Express 30(3), 4492-4503, Jan. 2022.

[24] S. Qiu, Q. Guo and Z. Li,“ Tunable Frequency Selective Surface Based on a Sliding 3D-Printed Inserted Dielectric,” in IEEE Access, 9, 19743- 19748, 2021.

[25] C. Cheng, Y. Lu, D. Zhang, F. Ruan, G. Li,“ Gain enhancement of terahertz patch antennas by coating epsilon-near-zero metamaterials,” Superlattices and Microstructures, 139, 106390, 2020.

[26] M. Chaluvadi, V. K. Kanth and K. G. Thomas,“ Design of a Miniaturized 2.5-D Frequency Selective Surface With Angular Incidence and Polarization Stability,” in IEEE Transactions on Electromagnetic Compatibility, 62(4), 4, 1068-1075, Aug. 2020.

[27] L. C. M. M. Fontoura, H. W. De Castro Lins, A. S. Bertuleza, A. G. D’assunc¸ao and A. G. Neto,“ Synthesis of Multiband Frequency ˜ Selective Surfaces Using Machine Learning With the Decision Tree Algorithm,” in IEEE Access, 9, 85785-85794, 2021.

[28] B. Li et al.,“ Bandpass Frequency Selective Structure With Improved Out of Band Rejection Using Stacked Single-Layer Slotlines,” in IEEE Transactions on Antennas and Propagation, 66(11), 6003-6014, Nov. 2018.

[29] H. F. Alvarez, D. A. Cadman, A. Goulas et al.,“ 3D conformal bandpass millimeter-wave frequency selective surface with improved fields of view,” Sci Rep 11, 12846, 2021.

[30] M. Harnois, M. Himdi, W. Y. Yong et al.,“ An Improved Fabrication Technique for the 3-D Frequency Selective Surface based on Water Transfer Printing Technology,” Sci Rep 10, 1714, 2020.

[31] R. A. Mellita, S. S. Karthikeyan and P. Damodharan,“ Additively Manufactured Conformal All-dielectric Frequency Selective Surface,” 50th European Microwave Conference (EuMC), 772-775, 2021.

[32] J. J. Peng, S. W. Qu, M. Xia and S. Yang,“ Conformal Phased Array Antenna for Unmanned Aerial Vehicle With ±70° Scanning Range,” in IEEE Transactions on Antennas and Propagation, 69(8), 4580-4587, Aug. 2021.

[33] G. Gerini and L. Zappelli,“ Multilayer array antennas with integrated frequency selective surfaces conformal to a circular cylindrical surface,” in IEEE Transactions on Antennas and Propagation, 53(6), 2020-2030, June 2005.

[34] A. Chatterjee and S. K. Parui,“ Frequency-Dependent Directive Radiation of Monopole-Dielectric Resonator Antenna Using a Conformal Frequency Selective Surface,” in IEEE Transactions on Antennas and Propagation, 65(5), 2233-2239, May 2017.

[35] K. K. Varikuntla, R. Singaravelu,“ Ultrathin design and implementation of planar and conformal polarisation rotating frequency selective surface based on SIW technology,” IET Microwaves, Antennas Propagation, 12(12), 0996, 2018.

[36] P. Das, K. Mandal,“ Modeling of ultra-wide stop-band frequency selective surface to enhance the gain of a UWB antenna,” IET Microwaves, Antennas Propagation, 13(3), 5426, 2019.

[37] V. A. A. Filho, A. L. P. S. Campos,“ Performance Optimization of Microstrip Antenna Array Using Frequency Selective Surfaces,” Journal of Microwaves, Optoelectronics and Electromagnetic Applications, 13(1), 31-46, march 2014.

[38] Q. Luo, S. Gao, M. Sobhy and X. Yang,“ Wideband Transmitarray With Reduced Profile,” in IEEE Antennas and Wireless Propagation Letters, 17(3), 450-453, March 2018.

[39] L. Z. Song, P. Y. Qin and Y. J. Guo,“ A High-Efficiency Conformal Transmitarray Antenna Employing Dual-Layer Ultrathin Huygens Element,” in IEEE Transactions on Antennas and Propagation, 69(2), 848- 858, Feb. 2021.

[40] X. Sheng, J. Fan, N. Liu and C. Zhang,“ A Miniaturized Dual-Band FSS With Controllable Frequency Resonances,” in IEEE Microwave and Wireless Components Letters, 27(10), 915-917, Oct. 2017.

[41] G. Xu, G. V. Eleftheriades and S. V. Hum,“ Generalized Synthesis Technique for High-Order Low-Profile Dual-Band Frequency Selective Surfaces,” in IEEE Transactions on Antennas and Propagation, 66(11), 6033-6042, Nov. 2018.

[42] S. Unaldi, N. B. Tesneli and S. Cimen,“ A Novel Miniaturized Polarization Independent Frequency Selective Surface with UWB Response,” Radio engineering, 27(4), 1012–1017, 2018.

[43] G. Xu, S. V. Hum and G. V. Eleftheriades,“ A Technique for Designing Multilayer Multistopband Frequency Selective Surfaces,” in IEEE Transactions on Antennas and Propagation, 66(2), 780-789, Feb. 2018.

[44] B. Li and Z. Shen,“ Dual-Band Bandpass Frequency-Selective Structures With Arbitrary Band Ratios,” in IEEE Transactions on Antennas and Propagation, 62(11), 5504-5512, Nov. 2014.

[45] D. Wang, W. Che, Y. Chang, K. Chin and Y. L. Chow,“ A Low-Profile Frequency Selective Surface With Controllable Triband Characteristics,” in IEEE Antennas and Wireless Propagation Letters, 12, 468-471, 2013.

[46] X.-D. Hu, X.-L. Zhou, L.-S. Wu, L. Zhou, and W.-Y. Yin,“ A miniaturized dual-band frequency selective surface (FSS) with closed loop and its complementary pattern,” IEEE Antennas Wireless Propag. Lett., 8, 1374–1377, Jan. 2010.

[47] Y. Yang, X.-H. Wang, and H. Zhou,“ Dual-band frequency selective surface with miniaturized element in low frequencies,” Prog. Electromagn. Res. Lett., 33, 167–175, Aug. 2012.

[48] G. Shan, C. Y. Gao, H. B. Pu and C. L. Chen,“ A Tri-Band Second order Frequency Selective Surface Designing and Analysis,” E3S Web Conf., 275, 0-3084, 2021.

[49] L. M. Lopez, R. M. Lopez, A. E. Martynyuk, J. R. Cuevas, H. F. Gongora and J. I. M. Lopez,“ Close Band Spacing Pentaband Frequency Selective Surfaces Based on Concentric Ring Slots,” in IEEE Access, 9, 57886- 57896, 2021.

[50] U. Mahaveer, K. T. Chandrasekaran, M. P. Mohan, A. Alphones, M. Y. Siyal and M. F. Karim,“ A tri-band Frequency-Selective Surface,” Journal of Electromagnetic Waves and Applications, 35(7), 861-873, 2021.

[51] S. Ghosh and K. V. Srivastava,“ An Angularly Stable Dual-Band FSS With Closely Spaced Resonances Using Miniaturized Unit Cell,” in IEEE Microwave and Wireless Components Letters, 27(3), 218-220, March 2017.

[52] V. K. Kanth and S. Raghavan,“ Design and optimization of complementary frequency selective surface using equivalent circuit model for wideband EMI shielding,” Journal of Electromagnetic Waves and Applications, 34(1), 51-69, Jan. 2020.

[53] X. Yuan, H. Mang,“ Design of Multilayer Frequency-Selective Surfaces by Equivalent Circuit Method and Basic Building Blocks,” International Journal of Antennas and Propagation, 1–13, 2019.

[54] X. Yao, M. Bai and J. Miao,“ Equivalent Circuit Method for Analyzing Frequency Selective Surface With Ring Patch in Oblique Angles of Incidence,” in IEEE Antennas and Wireless Propagation Letters, 10, 820-823, 2011.

[55] A. Firouzfar, M. Afsahi, A. A. Orouji,“ Novel, straightforward procedure to design square loop frequency selective surfaces based on equivalent circuit model,” AEU - International Journal of Electronics and Communications, 119, 153164, 2020.

[56] A. Chatterjee, S. K. Parui,“ A triple-layer dual-bandpass frequency selective surface of third order response with equivalent circuit analysis,” International Journal of RF and Microwave Computer-Aided Engineering, 30(2), e22047, 2020.

[57] X. Ma, Y. Liu, G. Wan and A. Pan,“ Angularly Stable Frequency Selective Surface Using Shifted Double-Sided Screens,” in IEEE Antennas and Wireless Propagation Letters, 19(7), 1192-1196, July 2020.

List of Publications

1. Presented paper titled " Dielectric Insertion effect on Frequency Selective Surfaces for Band Pass Filter design" in the IEEE International Conference on Distributed Computing and Electrical Circuits and Electronics (ICDCECE-2022) organized by ballari Institute of Technology and management, ballari, India in association with IEEE Bangalore section and IEEE Information Society on 23rd - 24th April, 2022.

2. Presented paper titled "Design of Dual Band Pass and Band Stop Frequency Selective Surface: For Wireless Communication " in the IEEE 2022 Trends in Electrical, Electronics, Computer Engineering Conference (*TEECCON-2022*)" (IEEE Conference Record# 54414) , organized by School of EEE, in association with IEEE Student Branch REVA UNIVERSITY, Technical Sponsored by IEEE Bangalore Section and IEEE Power & Energy Society Bangalore on 26th - 27th May, 2022.

3. Presented paper titled "Stable Gain With Frequency Selective Surface in Planar and Conformal Structure: For Radome Application " in the IEEE 2022 Trends in Electrical, Electronics, Computer Engineering Conference (*TEECCON-2022*)" (IEEE Conference Record# 54414) , organized by School of EEE, in association with IEEE Student Branch REVA UNIVERSITY, Technical Sponsored by IEEE Bangalore Section and IEEE Power & Energy Society Bangalore on 26th - 27th May, 2022.